*Am J Physiol Renal Physiol* 286: F617–F624, 2004.
First published November 18, 2003; 10.1152/ajprenal.00130.2003.

# Gentamicin traffics retrograde through the secretory pathway and is released in the cytosol via the endoplasmic reticulum

**Ruben M. Sandoval and Bruce A. Molitoris**

*Division of Nephrology, the Indiana Center for Biological Microscopy, Indiana University School of Medicine and the Roudebush Veterans Affairs Medical Center, Indianapolis, Indiana 46202*

Submitted 1 April 2003; accepted in final form 6 November 2003

**Sandoval, Ruben M., and Bruce A. Molitoris.** Gentamicin traffics retrograde through the secretory pathway and is released in the cytosol via the endoplasmic reticulum. *Am J Physiol Renal Physiol* 286: F617–F624, 2004. First published November 18, 2003; 10.1152/ajprenal.00130.2003.—Previous mechanisms describing how aminoglycosides exert their cellular toxicity, including lysosomal accumulation, rupture, and release, cannot account for the rapidity and extent of the observed subcellular and organ effects. Using immunoamplification techniques and colocalization with epitopes of the endoplasmic reticulum (ER), we report rapid retrograde transport of gentamicin to the ER. Additionally, exposure times of 2 and 4 h in LLC-$PK_1$ cells produced cytosolic release and nuclear association. Cellular internalization and trafficking of aminoglycoside structural analogs, amine-containing cationic fluorescent dextrans of 3,000 molecular weight, corroborated these findings. However, identical anionic fluorescent dextrans, or larger cationic dextrans, of 10,000 molecular weight, failed to traverse from the ER into the cytosol or localize within the nucleus. These studies suggest that a pathway exists that transports internalized aminoglycosides, and other small-molecular-weight cationic compounds, in a retrograde manner through the Golgi complex and to the ER. From there, these compounds move into the cytosol for delivery throughout the cell. To quantify the potential toxic effects of cytosolic aminoglycoside release, experiments examining mitochondrial membrane potential in the continued presence of extracellular gentamicin were undertaken and demonstrated a significant reduction after 4 and 8 h. These observations provide a mechanism for the rapidly induced known cellular alterations, including aberrant vesicle fusion, mitochondrial toxicity/free radical generation, and decreased protein synthesis either by reduced transcription or translation after aminoglycoside exposure.

endoplasmic reticulum; tyramide signal amplification; Texas red

GENTAMICIN IS A MEMBER OF the aminoglycoside family of antibiotics produced by the fungi *Micromonospora purpurea*. Although highly efficacious, these small molecular weight cationic compounds are associated with toxicity to the renal proximal tubule segment (2, 3, 8, 11, 23, 25, 27, 29). Uptake occurs via association with megalin or acidic phospholipids on the surface membrane in a low-affinity high-capacity fashion (12, 22, 24, 25, 31). For decades, uptake and trafficking were believed to shuttle the compound via the endocytic route entirely to lysosomes. Consequently, toxicity had been relegated to lysosomal rupture, cytosolic release, and permeation to adjacent cells via gap junctions. Studies conducted to investigate alterations in protein synthesis and other cellular perturbations concluded that these alterations were occurring much too rapidly, in the proposed "blueprint" of toxicity, to be accounted for by lysosomal accumulation, rupture, and release (2, 3). Unfortunately, many of the protocols developed to conduct these studies relied on cell fractionation techniques (13, 32). Therefore, pundits of the established mechanism relegated these observations to artifacts of lysosomal rupture and nonspecific association with intracellular organelles during the experimental protocol.

Using a previously characterized form of gentamicin conjugated to Texas Red (TRG), we have shown up to 10% of the internalized TRG compound traffics rapidly and directly to the Golgi complex (17, 18, 19). We postulated that this organelle could act as a hub and shuttle gentamicin to other intracellular compartments, resulting in the rapid initiation of a myriad of cytotoxic effects. Therefore, the present study was conducted to follow more distal routes of gentamicin handling and intracellular accumulation at longer time points. We employed confocal microscopy to follow both fluorescently labeled and immunolocalized gentamicin. We also utilized a previously described technique to neutralize the signal from both fluorescent and nonfluorescent gentamicin emanating from the lysosomal pool (14, 16, 18, 19). This protocol markedly improved the signal-to-noise ratio of nonlysosomal gentamicin.

Results from these studies revealed rapid accumulation within the endoplasmic reticulum (ER). Moreover, after 2 and 4 h of continual administration, cytosolic release and subsequent nuclear association occurred with both the fluorescent and nonfluoresent forms of gentamicin. This observation also occurred with structural analogs (small-molecular-weight, amine-containing, cationic, fluorescent dextrans). Monitoring mitochondrial potential in LLC-$PK_1$ cells, under continual exposure to gentamicin, revealed a steady decline therein, with a significant reduction in membrane potential after 4 and 8 h of exposure.

Taken together, these data suggest aminoglycosides, like other cellular toxins such as cholera and ricin, traffic retrograde from the endocytic route and are released in the cytosol (9, 20, 21). We postulate export to the cytosol allows association with various intracellular organelles to induce a multitude of events leading to proximal tubule injury.

## MATERIALS AND METHODS

*Experimental model.* Porcine kidney proximal tubule cells (LLC-$PK_1$; ATCC, Rockville, MD) were grown on 18-mm-diameter coverslips (Fisher Scientific, Itasca, IL) for colocalization experiments. Cells were maintained in K-P media, a 1:1 mixture of DMEM and Ham's nutrient mixture (F-12), supplemented with 10% FBS and 1

Address for reprint requests and other correspondence: B. A Molitoris, Indiana Univ. School of Medicine, 950 West Walnut, R2-E251, Indianapolis, IN 46202 (E-mail: bmolitor@iupui.edu).

The costs of publication of this article were defrayed in part by the payment of page charges. The article must therefore be hereby marked "*advertisement*" in accordance with 18 U.S.C. Section 1734 solely to indicate this fact.

mg/ml penicillin-streptomycin (Sigma, St. Louis, MO). Cells were allowed to reach a state of ~40–70% confluence before being used in experimental protocols (17–19).

*Lysosomal fluorescence quenching and TRG uptake studies.* Lysosomal and endosomal fluorescence was quenched as previously described (6, 14, 16, 19). This reaction also prevents association of anti-gentamicin antibodies to pools within these structures. After preincubation in media containing horseradish peroxidase (HRP), cells were placed in K-P media containing 2 mg/ml TRG (Molecular Probes, Eugene, OR) for 1, 2, or 4 h. Cells were then washed two times briefly in PBS and fixed in freshly thawed 4% paraformaldehyde in PBS, pH 7.4, for 1 h at room temperature or at 4°C overnight.

*Immunolocalization and amplification of nonfluorescent gentamicin.* After HRP uptake, cells were allowed to accumulate gentamicin (Fluka, Ronkonkama, NJ) in media containing 1 mg/ml gentamicin for either 15, 30, or 60 min or 2 or 4 h. After fixation, the cells were processed following the lysosomal fluorescence quenching protocol, as we have described previously (19). Next, cells were incubated in 1% $H_2O_2$ in PBS for 20 min to quench any residual HRP activity. This was necessary as the amplification protocol is HRP dependent and residual HRP activity from lysosomes would obscure the results. The cells were processed via the tyramide signal amplification (TSA) protocol known to increase sensitivity up to 1,000-fold (formerly NEN Life Sciences, now PerkinElmer) to produce a red fluorescence, as previously reported (26). The primary antibody goat-anti-gentamicin (Hyclone, Logan, UT) was used at a 1:500 dilution in the proprietary blocking buffer provided. The HRP-conjugated donkey-anti-goat secondary antibody (Jackson ImmunoResearch, West Grove, PA) was used at a 1:1,000 dilution.

*Immunolocalization of the ER.* After TSA gentamicin localization, the cells were processed routinely for immunolocalization of the ER using a monoclonal antibody against the *Dolichos*-phosphate mannose synthase epitope (Molecular Probes) diluted at 1:50 in a PBS blocking buffer containing 2% BSA (Sigma). The FITC-conjugated sheep-anti-mouse secondary antibody (Jackson ImmunoResearch) was used at a 1:200 dilution in blocking buffer.

*Fluorescent dextran uptake.* To investigate the phenomena of cytosolic release, small-molecular-weight amine-containing dextrans, postulated to be structural analogs of TRG, were used at 1 or 2 mg/ml in normal media for 2 h. These included 3,000 molecular weight Texas red lysine conjugated (cationic), 3,000 molecular weight FITC lysine conjugated (anionic), 3,000 molecular weight rhodamine lysine conjugated (anionic), and 10,000 molecular weight Texas red lysine conjugated (cationic), all purchased from Molecular Probes.

*Mitochondrial potential.* To determine whether the cytosolic release of gentamicin was cytotoxic, mitochondrial potential was studied. Briefly, three groups on coverslips with LLC-$PK_1$ cells were incubated at 1 mg/ml gentamicin for 2, 4, and 8 h. The cells were placed in K-P media containing 0.1 μg/ml rhodamine B, hexyl ester (Molecular Probes), for 8 min and then placed in K-P media (30). Cells were then mounted on coverslip bottom dishes with K-P media, and images were collected. Ten confluent fields per coverslip were collected for a total of 30 fields/group. The images were background

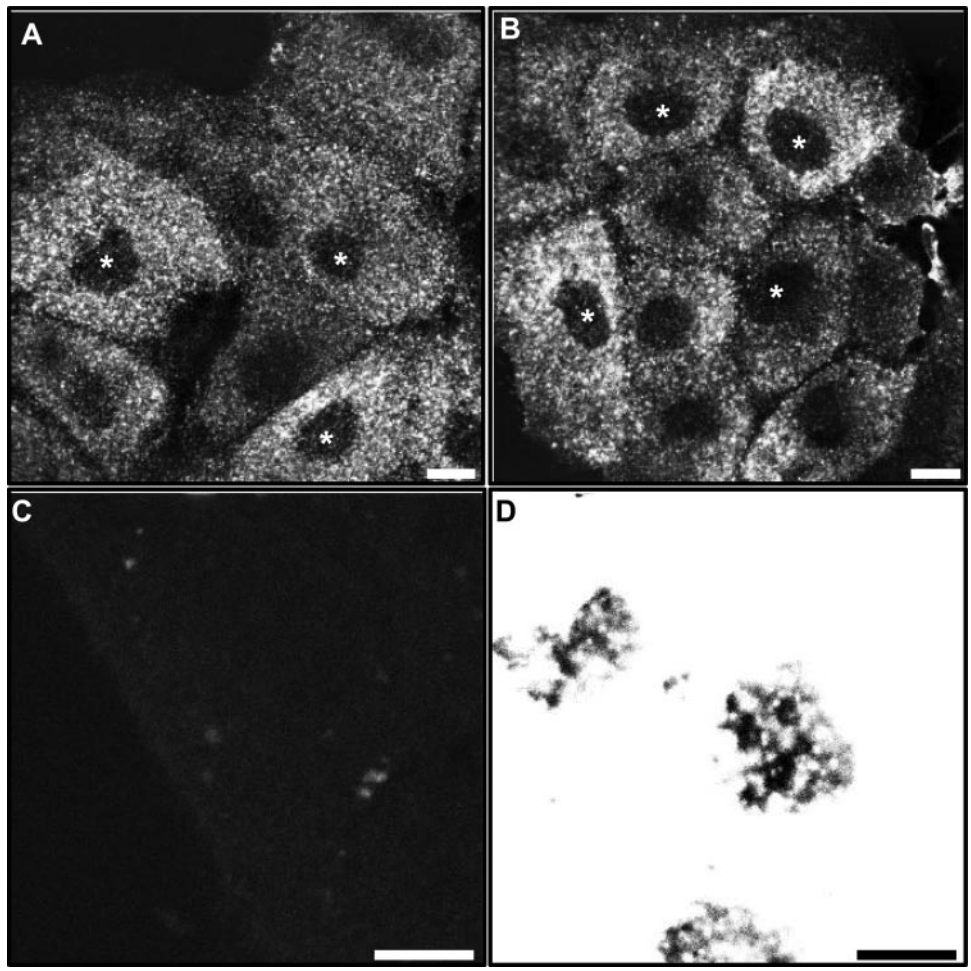


Fig. 1. Immunoamplification of native gentamicin produces a reticular staining pattern present throughout the entire cytosol of LLC-$PK_1$ cells. Continuous exposure to native gentamicin for 15 and 30 min (*A* and *B*, respectively) produced a staining pattern confined within a distinct reticulum, extending throughout the cell. Prevalent is the absence of any fluorescence within the nucleus (*). *C*: control cells incubated with secondary antibody only, or stained without exposure to gentamicin, failed to produce any discernable fluorescence. *D*: when the lysosomal quenching protocol was omitted, and acquisition parameters were kept constant, fluorescence intensity overwhelmed the microscope detectors, causing saturation and blooming. Bar = 10 μm.

subtracted, and an average intensity from the 10 fields was used to generate a mean intensity to give an *n* of 3 for the stated time points. Results in the corresponding graph are expressed as percent control values ± SD.

*Image acquisition.* Images were acquired on a Bio-Rad (Hercules, CA) MRC-1024 combination 2-photon, *trans*-illumination capability, Kr/Ar Laser Scanning Confocal Microscope on a Nikon Diaphot inverted microscope platform using either a ×100 oil immersion objective with a numeric aperture (NA) of 1.4 or a ×60 water immersion objective with an NA of 1.2. To avoid the possibility of spectral overlap in the colocalization studies, the signals from the Texas red and FITC emissions were excited and acquired sequentially using the Kr/Ar laser in single photon mode.

*Image analysis and processing.* All of the experimental protocols were repeated a total of three times to replicate findings. The images from the colocalization studies were processed and overlaid using Metamorph version 4.0 image processing software (Universal Imaging, West Chester, PA). Lateral or *X-Z* projections were generated from fields where through focus optical sections were taken.

*Statistical analysis.* Average intensity measurements from the mitochondrial potential experiment were analyzed using a Student's *t*-test. Statistical significance was attained with $P$ values $\leq 0.05$.

## RESULTS

Initial studies were conducted to investigate intracellular accumulation and distribution of gentamicin using highly sensitive amplification techniques. Gentamicin internalized in LLC-PK$_1$ cells exhibited a reticular staining pattern within as early as 15 min of uptake (Fig. 1*A*) and remained consistent at time points of 30 min (Fig. 1*B*). For both time points, the signal was confined to this defined reticular pattern and absent from the nucleus. The up to 1,000-fold increase in fluorescence generated by the TSA protocol elucidated the reticular staining pattern not previously seen by using the Lysosomal Quenching protocol and TRG (18, 19). Control slides treated with either primary and secondary antibody in the absence of gentamicin, or gentamicin and secondary antibody only, demonstrated the pattern was not due to some artifact of nonspecific staining or processing (Fig. 1*C*). Also, omission of the lysosomal quenching protocol, processing for TSA amplification, and image acquisition under identical parameters produced fluorescence so intense that saturation and blooming occurred and completely obscured any discernible signal (Fig. 1*D*). This micrograph serves to underscore the importance of removing any fluorescence or blocking immunolocalization of gentamicin within the lysosome.

A high degree of colocalization was observed after costaining of the amplified immunolocalized native gentamicin, internalized for 60 min, and the ER epitope *Dolichos*-phosphate mannose synthase. When regions of gentamicin labeling using a secondary antibody (Fig. 2*A*, in red) are merged with the ER marker (Fig. 2*B*, in green), the resulting overlaid images (Fig 2,

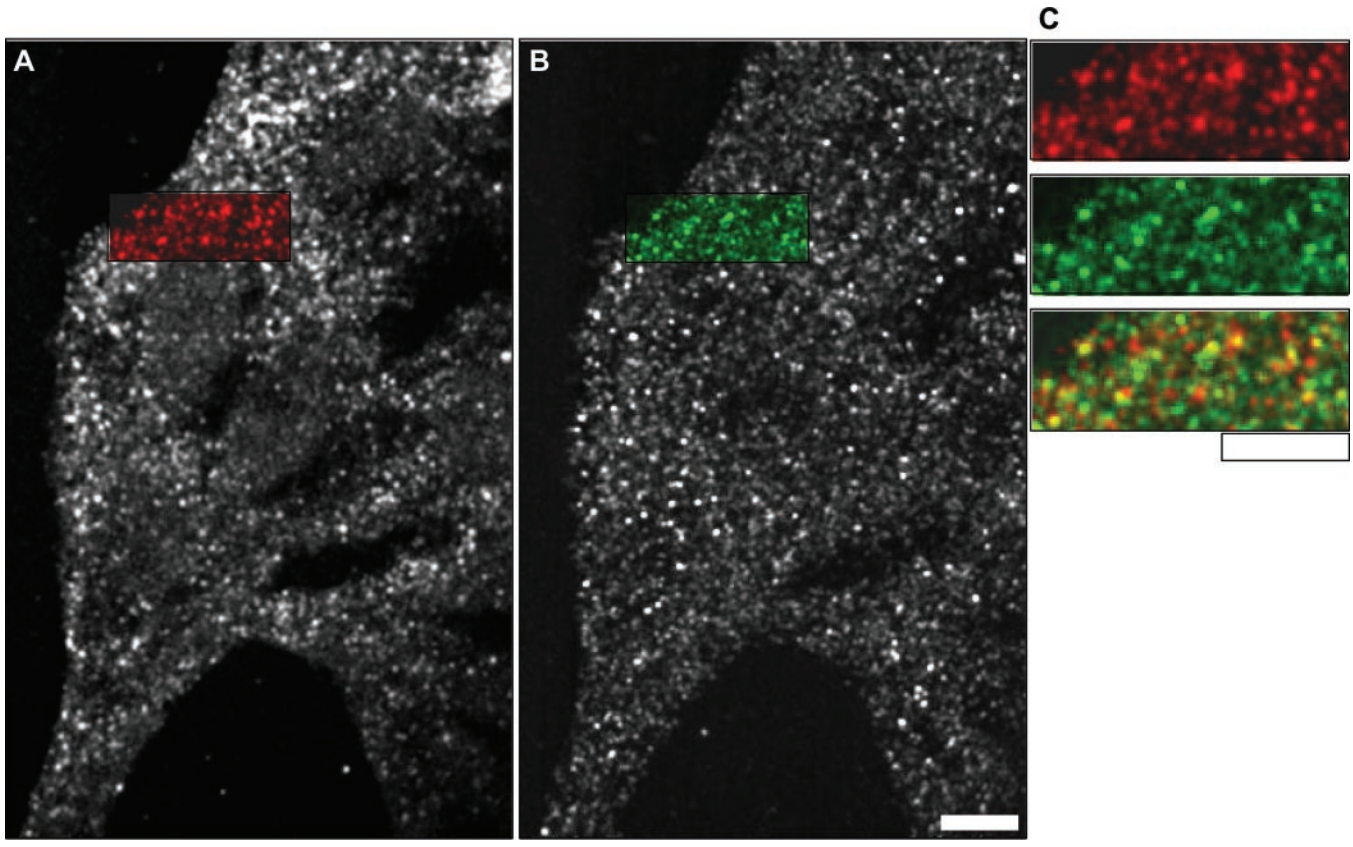


Fig. 2. Gentamicin colocalizes with the endoplasmic reticulum (ER) epitope *Dolichos*-phosphate mannose synthase. LLC-PK$_1$ cells were exposed to gentamicin for 30 min and fixed and processed using the TSA protocol. The cells were then stained for gentamicin and the ER marker and evaluated for colocalization. Areas from the gentamicin (*A*, red) and ER (*B*, green) signal were color encoded, enlarged, and merged to display colocalization (*C*). In all micrographs, a reticular staining pattern consistent with ER morphology was discernable. Bar = 10 μm.

*C* and *D*) exhibit the characteristic yellow overlay color in areas of equal intensity.

When internalization was allowed to occur for 2 and 4 h, a gradual diffuse cytosolic staining pattern for the TSA-localized gentamicin occurred. At 60 min of uptake (Fig. 3*A*), staining was confined within the reticular pattern and excluded from the nucleus. At 2 h of exposure (Fig. 3*B*) an early trend toward diffuse cytosolic labeling occurred, with the nucleus now showing labeling as well. By 4 h (Fig. 3*C*), the cytosolic distribution was more apparent, and the nucleus exhibited the same fluorescence intensity as the cytosol. The same staining pattern occurred when LLC-$PK_1$ cells were incubated in TRG without TSA amplification. After 2 h uptake, a diffuse cytosolic labeling also appeared with movement in the nucleus (Fig. 3*D*). Describing an association with the ER is crucial in helping explain rapidly occurring alterations in protein synthesis, believed to be an important factor in the initial stages of toxicity. One observation noted in this present study was the lack of Golgi staining seen when employing the TSA protocol. In our previous publication utilizing TRG (19 and see Fig. 5), cells were grown on etched coverslips, and sequential images of the same areas were collected for colocalization analysis after *1*) fixation, *2*) lysosomal quenching, *3*) staining of the trans-Golgi network/trans-Golgi with the membrane dye C6-NBD ceramide, and *4*) permeabilization with Triton X-100 and staining of the Cis/medial Golgi with a fluorescein-conjugated lectin from *Lens culinaris*. A marked decrease in TRG fluorescence was noted after a single permeabilization step. The TSA protocol in the present study utilized a wash buffer containing Tween 20 in all washes. This repeated exposure to detergent likely removed all of the membrane-bound gentamicin, leaving only the protein-bound pool behind. Gentamicin bound to export channels in the ER, or closely linked to membrane proteins, would resist being washed away.

To test the shuttling hypothesis of cationic compounds in the cytosol after endocytic uptake, trafficking of small-molecular-weight amine-containing dextrans was examined. A cationic 3,000-molecular-weight lysine-conjugated dextran labeled with Texas red reached the cytosol and nuclei after 2 h of continual administration (Fig. 4*A*). However, a cationic 10,000-molecular-weight lysine-conjugated dextran labeled with Texas red (Fig. 4*B*) failed to reach the cytosol and nucleus. In addition, anionic derivatives of the 3,000-molecular-weight dextran, labeled with either tetramethyl rhodamine or fluorescein (Fig. 4, *C* and *D*, respectively), also remained sequestered within the endosomal compartment. The distribution of the anionic forms appeared more evenly distributed in these punctate vesicles throughout the cell compared with the cationic form in Fig. 4*A*, which appeared much more perinuclear in the majority of cells. Images at different focal planes

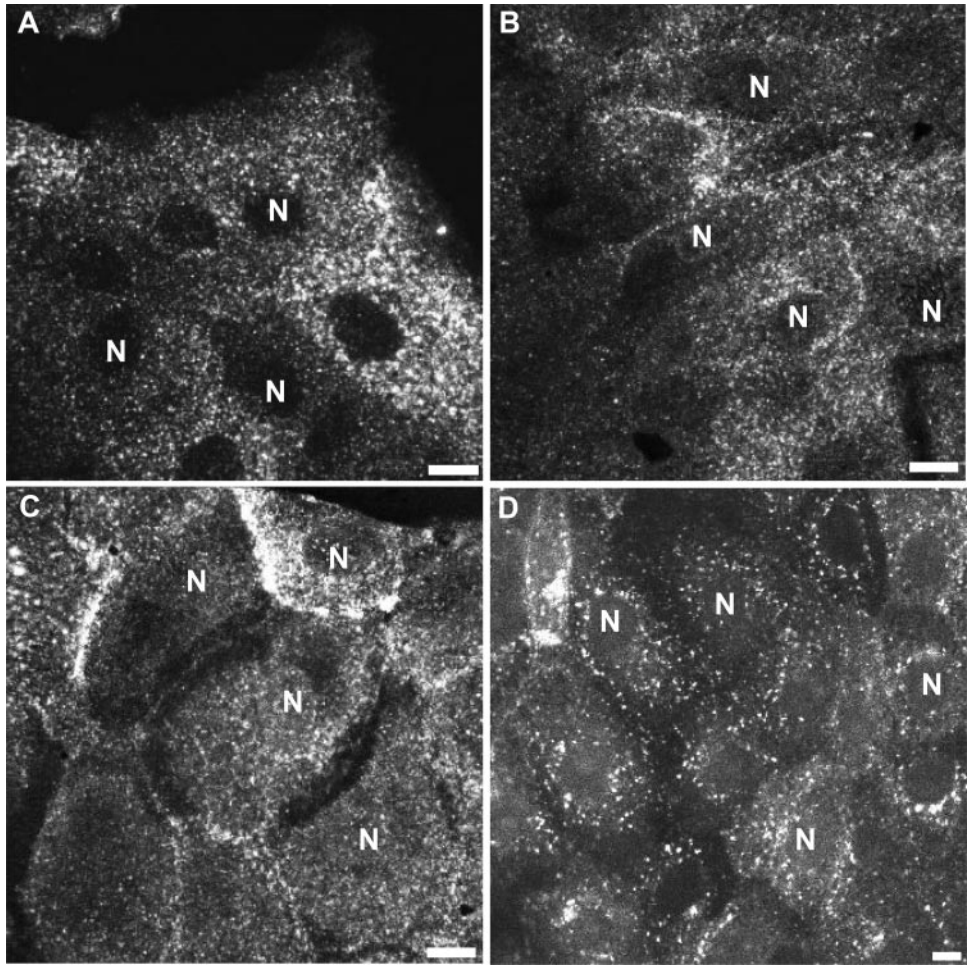


Fig. 3. Exposure to native gentamicin resulted in cytosolic release and nuclear accumulation in LLC-$PK_1$ cells. *A*: a reticular staining pattern was seen for exposure times of up to 1 h in TSA-immunoamplified cells. There was also no signal associated with the nuclei (N). *B*: at 2 h of exposure, a fluorescent cytosolic labeling began to emerge, as well as some early accumulation within the nuclei (N). *C*: by 4 h of exposure, the diffuse cytosolic signal was more prominent, and nuclei are no longer easily distinguishable from the cytosol. *D*: the same cytosolic and nuclear labeling occurred with the Texas red conjugate of gentamicin after 2 h of exposure. The punctate staining pattern seen in *D* is the result of the fluorescence of lysosomal-associated TRG, which had not been quenched in this photomicrograph. Bar = 10 μm.

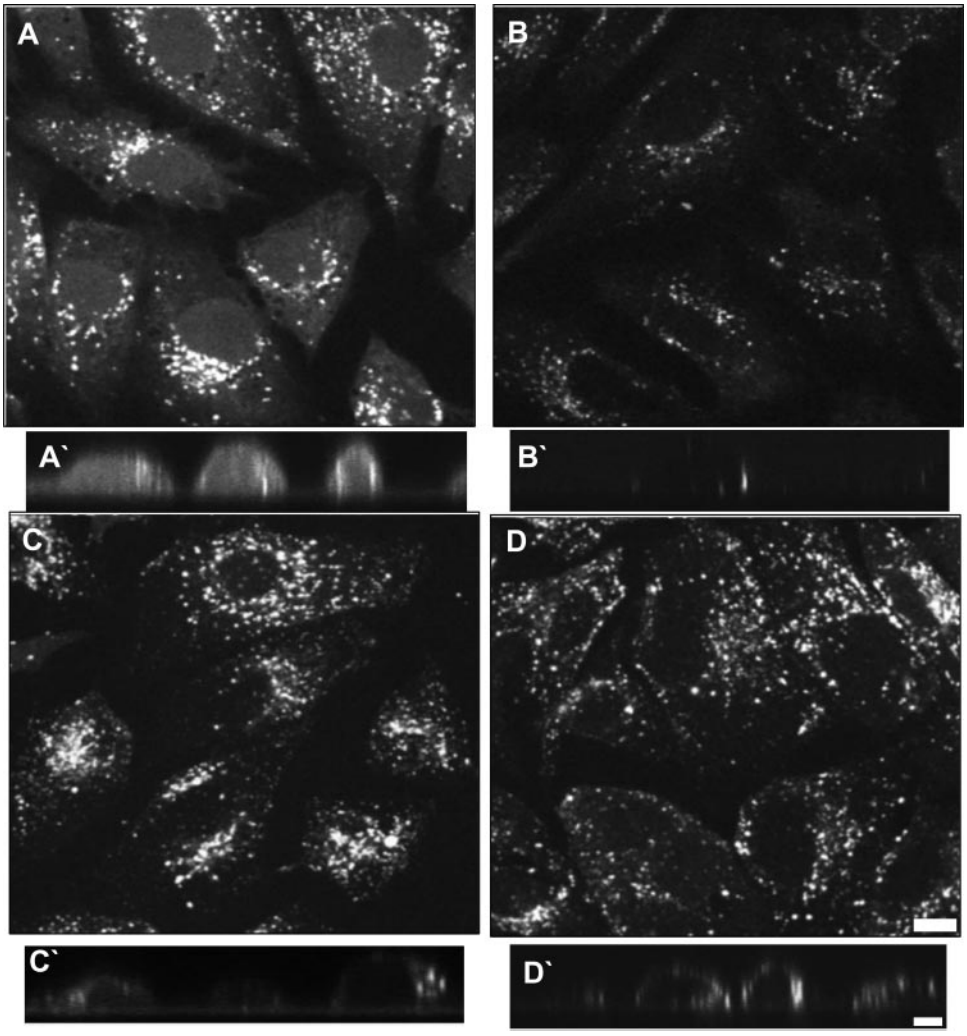


Fig. 4. Small-molecular-weight cationic dextrans, potential structural analogs of gentamicin, allowed to accumulate for 2 h in LLC-PK$_1$ translocated in the cytosol and accumulated in nuclei. Small 3,000-molecular-weight cationic lysine-conjugated dextrans labeled with Texas red (*A* and *A′*) or anionic labeled with tetramethyl rhodamine (*C* and *C′*) or fluoresce (*D* and *D′*) exhibited different staining patterns. *A*: the small-molecular-weight cationic dextran localized within the cytosol and the nuclei. *B*: a larger 10,000-molecular-weight lysine-conjugated cationic dextran labeled with Texas Red failed to translocate into the cytosol, suggesting export may be size dependent. *C* and *D*: the small-molecular-weight anionic dextrans remained sequestered within punctate vesicular structures. *A′*, *B′*, *C′*, and *D′*: lateral projections constructed from optical sections show apical domains at *top* and basolateral domains at *bottom*. The nuclei of the small anionic dextrans (*C′* and *D′*) and the large cationic dextran (*B′*) can be distinguished by the lack of fluorescence accumulation. *A′*: in the small cationic dextran, the nuclei clearly show accumulation of the fluorescent dextran. Bar = 10 μm.

were also collected at defined intervals, and lateral or *X-Z* projections were constructed for each of the dextrans (Fig. 4, *A′*, *B′*, *C′*, and *D′*). In projections of the anionic (Fig. 4, *C′* and *D′*) and 10,000-molecular-weight cationic form (Fig. 4*B′*), the nucleus was demarcated by exclusion of fluorescence. In the 3,000-molecular-weight cationic form (Fig. 4*A′*), the location of the nucleus is not as readily apparent because of labeling with the fluorescent dextran.

Having demonstrated cytosolic release of gentamicin and small cationic dextrans, we next chose to examine potential biological effects of cytosolic gentamicin in the cytosol as a test of cell toxicity. Because the association of gentamicin with mitochondrial membranes would likely alter membrane potential quickly, we studied rhodamine B hexyl ester mitochondrial labeling as a measure of mitochondrial potential. Typical mitochondrial staining under physiological conditions was manifested throughout the cytosol, with some heterogeneity in intensity between cells (Fig. 5*A*). Exposure to gentamicin for 2, 4, and 8 h (Fig. 5, *B*, *C*, and *D*, respectively) produced a stark decrease in mitochondrial membrane potential. Ten confluent fields were chosen and quantified for fluorescence. The average fluorescence intensity of the vital dye, directly proportional to mitochondrial membrane potential, was graphed in Fig. 6. A steady reduction in fluorescence compared with values under physiological conditions is observed, with significant decreases occurring after 4 and 8 h of exposure to 1 mg/ml gentamicin.

## DISCUSSION

The transport of materials in a retrograde manner from the endocytic pathway through the Golgi complex and to the ER has been implicated as a mechanism by which some toxins exert their detrimental effects (9, 20, 21). Most recently, cholera toxin from *Vibrio cholerae*, upon reaching the ER via this pathway, interacts with protein disulfide isomerase in the ER and subsequently translocates to the cytosol via the Sec61p channel (7, 15). In addition, a direct route from the cell surface to ER via caveolae has been described (4). Our studies did not rule out the possibility that this pathway augmented the ER-associated pool.

Because our previous work documented rapid direct trafficking of TRG to the Golgi complex after internalization, we next sought to further characterize intracellular destinations. The long-standing model for nephrotoxicity associated with

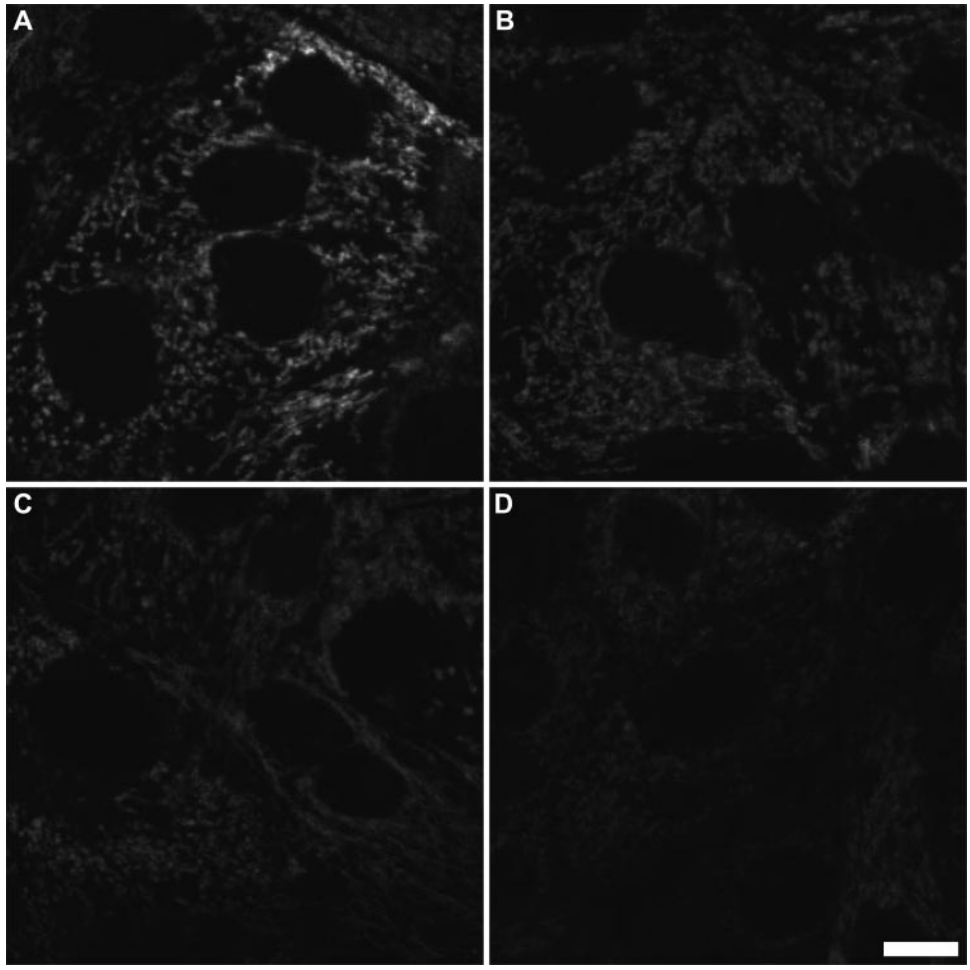


Fig. 5. LLC-PK$_1$ cells exposed continuously to gentamicin exhibit a decrease in mitochondrial potential. Cells were incubated in physiological media alone (*A*) or media containing 1 mg/ml gentamicin for 2 (*B*), 4 (*C*), or 8 (*D*) h. Cells were then incubated in physiological media containing 0.1 μg/ml of the potentiometric dye rhodamine B, hexyl ester for 8 min and imaged intravitally using confocal microscopy. *A*: photomicrographs show typical mitochondrial staining and morphology in the untreated group, with a large empty space in the center of the cell representing the nuclear area. *B–D*: exposure to gentamicin decreased fluorescence intensity. All the fields in these micrographs are of confluent areas within the cell monolayer and were imaged using identical acquisition parameters. Bar = 10 μm.

aminoglycosides has been centered around lysosomal accumulation. The novel observation that the Golgi complex acts as a "hub" and shuttles gentamicin-containing vesicles to other organelles can account for some, but not all, subsequent alterations.

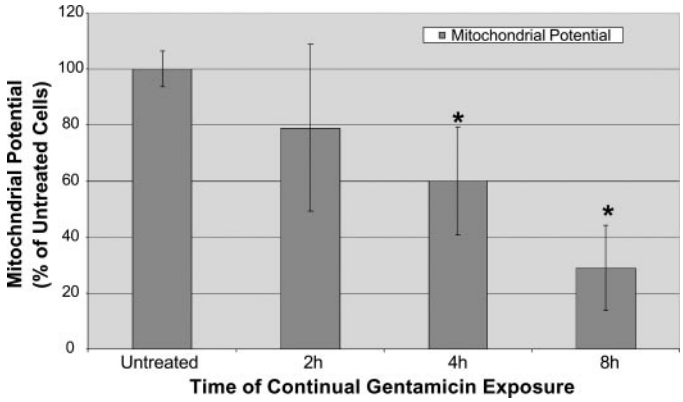


Fig. 6. Mitochondrial potentials show a progressive reduction with gentamicin exposure. Images from 10 random fields of confluent cells incubated with the mitochondrial potential dye rhodamine B were background subtracted, and the average intensity was calculated. Values are represented as %control ± SD. After 4 and 8 h of gentamicin exposure, a significant decrease in mitochondrial potential was detected (*$P \leq 0.05$).

The observation of cytosolic release, seen with both the native and fluorescent forms of gentamicin, could potentially account for many of the observed mechanisms of cytotoxicity (Fig. 7). For example, the known decrease in protein synthesis can now be attributed to gentamicin association with the ER and Golgi complex and also with the DNA in the nucleus reducing transcription. Additionally, association of gentamicin directly with membrane domains facing the cytosol could explain vesicle fusion perturbations and alterations in mitochondrial potential and subsequent free radical generation (11, 27, 29). Necrosis and apoptosis studies conducted in our laboratory using time points and concentrations identical to this study confirmed that this mechanism occurs in viable cells and that the observation of cytosolic release is not the result of events immediately preceding cell death and lysosomal rupture (18).

Studies conducted with the fluorescent dextrans provide additional corroborative evidence implicating ER association and release of small cations in the cytosol. The findings suggest these small-molecular-weight cationic compounds are exploiting a naturally occurring mechanism to reach their eventual destination within the cytosol. Suspect channels include channels located within the ER that translocate small glycopeptides, carbohydrates, and misfolded proteins to the cytosol, the latter for degradation by proteosomes (7, 15). The unique structure of

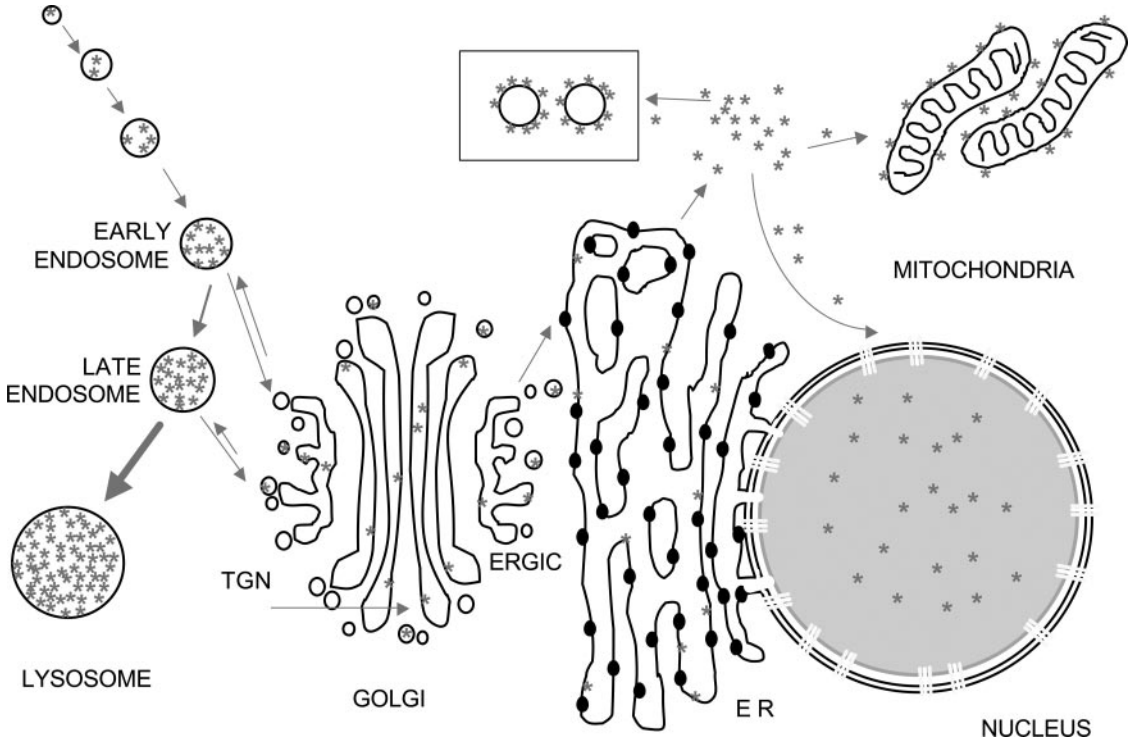


Fig. 7. Diagram showing the route of retrograde trafficking along the endocytic pathway taken by gentamicin in LLC-PK$_1$ cells. Internalization occurs via receptor-mediated endocytosis with ~90% of the internalized material accumulating within lysosomes. However, ~10% is shuttled to the Golgi complex and is transported past the ER-Golgi intermediate compartment (ERGIC) to the ER. From there, translocation to the cytosol occurs. Once in the cytosol, association with various organelles such as the outer mitochondrial membranes and nuclei can initiate an additional cascade of events leading to renal proximal tubule injury. These data may explain previous observations showing mitochondrial localization, free radical formation, and alterations in mitochondrial function (11, 27, 29).

gentamicin, a three-ring O-linked carbohydrate moiety decorated with primary amine groups, is well suited to exploit translocation mechanisms where recognition factors are carbohydrate and/or protein based. In the present studies, there was an apparent size and charge requirement for ER translocation in the cytosol.

The decrease in mitochondrial potential described in this study may indeed represent one of the earliest cytotoxic effects gentamicin imparts on the proximal tubule cell. Alterations in mitochondrial potential correlate closely with the observed phenomena of cytosolic release. After 2 h of exposure, some evidence of cytosolic release was seen in both native and fluorescent gentamicin studies (Fig. 3, *B* and *D*, respectively); at this time, a decrease, although not significant, is seen in mitochondrial potential. After 4 h of exposure, gentamicin is readily seen within the cytosol and nucleus in all cells (Fig. 3*C*), and the decrease in mitochondrial potential at this time point becomes significant. This observed decrease continues at 8 h of exposure and begins to rebound after 24 h of exposure (data not shown).

In summary, we describe a novel mechanism for the rapid retrograde transport of gentamicin along the secretory pathway to the ER. Once there, its unique structure may play an important role in translocation across the ER membrane and in the cytosol, a phenomena that seems to be size and charge dependent. The characterization of this pathway may provide a mechanism that accounts for many of the reported subcellular cytotoxicities occurring within the renal proximal tubule associated with animoglycoside nephrotoxicity.

## REFERENCES

1. **Beauchhamp D, Gourde P, and Bergeron MG.** Subcellular distribution of gentamicin in proximal tubular cells, determined by imunogold labeling. *Antimciron Agents Chemother* 35: 2173–2179, 1991.
2. **Bennett WM, Mela-Riker LM, Houghton DC, Gilbert DN, and Buss WC.** Microsomal protein synthesis inhibition: an early manifestation of gentamicin nephrotoxicity. *Am J Physiol Renal Fluid Electrolyte Physiol* 255: F265–F269, 1988.
3. **Buss WC and Piatt MK.** Gentamicin administered in vivo reduces protein synthesis in microsomes subsequently isolated from rat kidney but not from rat brain. *J Antimicrob Chemother* 15: 715–721, 1985.
4. **Conrad PA, Smart EJ, Ying YS, Anderson RG, and Bloom GS.** Caveolin cycles between plasma membrane caveolae, and the Golgi complex by microtubule-dependent and microtubule-independent steps. *J Cell Biol* 131: 1421–133, 1995.
5. **Ford DM, Dahl RH, Lamp CA, and Molitoris BA.** Apically and basolaterally internalized aminoglycosides co-localize in LLC-PK$_1$ lysosomes and alter cell function. *Am J Physiol Cell Physiol* 266: C52–C57, 1994.
6. **Futter CE, Pearse A, Hewlett LJ, and Hopkins CR.** Multivesicular endosomes containing internalized EGF-EGF receptor complexes mature, and then fuse directly with lysosomes. *J Cell Biol* 132: 1011–1023, 1996.
7. **Gillece P, Pilon M, and Romisch K.** The protein translocation channel mediates glycopeptide export across the endoplasmic reticulum membrane. *Proc Natl Acad Sci USA* 97: 4609–4614, 2000.
8. **Hammond TG, Majewski RR, Kaysen JH, Goda FO, Navar GL, Pontillon F, and Verroust PJ.** Gentamicin inhibits rat renal cortical homotypic endosomal fusion: role of megalin. *Am J Physiol Renal Physiol* 272: F117–F123, 1997.

9. **Lord JM and Roberts LM.** Toxin entry: retrograde transport through the secratory pathway. *J Cell Biol* 140: 733–736, 1998.
10. **Luetterforst R, Stang E, Zorzi N, Carozzi A, Way M, and Parton RG.** Molecular characterization of cavelin association with the Golgi complex: Identification of a Cis-Golgi targeting domain in the Caveolin molecule. *J Cell Biol* 147: 1443–1459, 1999.
11. **Mela-Riker LM, Widener LL, Houghton DC, and Bennet WM.** Renal mitochondrial integrity during continuous gentamicin treatment. *Biochem Pharmacol* 35: 979–984, 1986.
12. **Moestrup SK, Shiying C, Vorum H, Bregengard C, Bjorn SE, Norris K, Gliemann J, and Crhistensen EI.** Evidence that epithelial glycoprotein 330/megalin mediates uptake of polybasic drugs. *J Clin Invest* 96: 1404–1413, 1995.
13. **Nassberger L, Bergstrand A, and DePierre JW.** Intracellular distribution of gentamicin within the rat kidney cortex: a cell fractionation study. *Exp Mol Pathol* 52: 212–220, 1990.
14. **Odorizzi G, Pearse A, Domingo D, Trowbridge IS, and Hopkins CR.** Apical, and basolateral endosomes of MDCK cells are interconnected and contain a polarized sorting mechanism. *J Cell Biol* 135: 139–152, 1996.
15. **Romisch K.** Surfing the Sec61 channel: bi-directional protein translocation across the ER membrane. *J Cell Sci* 112: 4185–4191, 1999.
16. **Sandell JH and Masland RH.** Photoconversion of some fluorescent markers to a diaminobenzidine product. *J Histochem Cytochem* 36: 555–559, 1988.
17. **Sandoval R, Leiser J, and Molitoris BA.** Aminoglycoside antibiotics traffic to the Golgi Complex in LLC-$PK_1$ cells. *J Am Soc Nephrol* 9: 167–174, 1998.
18. **Sandoval RM, Bacallao RL, Dunn KW, Leiser JD, and Molitoris BA.** Nucleotide depletion increases trafficking of gentamicin to the Golgi complex in LLC-$PK_1$ cells. *Am J Physiol Renal Physiol* 283: F1422–F1429, 2002.
19. **Sandoval RM, Dunn KW, and Molitoris BA.** Aminoglycosides traffic rapidly, and directly to the Golgi complex in LLC-$PK_1$ cells. *Am J Physiol Renal Physiol* 279: F884–F890, 2000.
20. **Sandvig K, Garred O, Helvoort A, van Meer G, and van Deurs B.** Importance of glycolipid synthesis for butyric acid-induced sensitization to Shiga toxin, and intracellular sorting of toxin in A431 cells. *Mol Biol Cell* 7: 1391–1404, 1996.
21. **Sandvig K, Ryd M, Oystern G, Schweda E, Holm PK, and vanDeurs B.** Retrograde transport from the Golgi complex to the ER of both Shiga toxin, and the nontoxic Shiga b-fragement is regulated by butyric acid and cAMP. *J Cell Biol* 126: 53–64, 1994.
22. **Sastrasinh M, Knauss TC, Weinberg JM, and Humes HD.** Identification of aminoglycoside binding site in rat renal brush border membranes. *J Pharmacol Exp Ther* 222: 350–358, 1982.
23. **Schentag JJ, Plaut ME, and Cerra FB.** Comparative nephro-toxicity of gentamicin and tobramycin: pharmacokinetic and clinical studies in 201 patients. *Antimicrob Agents Chemother* 19: 859–866, 1981.
24. **Silverblatt FJ and Kuehn C.** Autoradiography of gentamicin uptake by the rat proximal tubule cell. *Kidney Int* 15: 335–345, 1979.
25. **Sundin DP, Sandoval R, and Molitoris BA.** Gentamicin inhibits renal protein, and phospholipid metabolism in rats: implications involving intracellular trafficking. *J Am Soc Nephrol* 12: 114–123, 2001.
26. **Toda Y, Kono K, Abiru H, Kokuryo K, Endo M, Yaegashi H, and Fukumoto M.** Application of tyramide signal amplification to immunohistochemistry: a potent method to localize antigens that are not detectable by ordinary methods. *Pathol Int* 49: 479–483, 1999.
27. **Ueda N, Guidet B, and Shah SV.** Gentamicin-induced mobilization of iron from renal cortical mitochondria. *Am J Physiol Renal Fluid Electrolyte Physiol* 265: F435–F439, 1993.
28. **Verkade P, Harder T, Lafont F, and Simons K.** Induction of caveolae in the apical plasma membrane of Madin-Darby canine kidney cells. *J Cell Biol* 148: 727–739, 1999.
29. **Walker PD and Shah SV.** Gentamicin enhanced production of hydrogen peroxide by renal cortical mitochondria. *Am J Physiol Cell Physiol* 234: C495–C499, 1978.
30. **Wang YL and Taylor DL.** *Methods in Cell Biology: Fluorescence Microscopy fo Living Cells in Culture*. New York: Academic, vol. 29, 1989.
31. **Wedeen RP, Batuman V, Cheeks C, Marquet E, and Sobel H.** Transport of gentamicin in rat proximal tubule. *Lab Invest* 48: 212–223, 1983.
32. **Weinberg JM, Hunt D, and Humes HD.** Distribution of gentamicin among subcellular fractions from rat renal cortex. *Biochem Pharmacol* 34: 1779–1787, 1985.